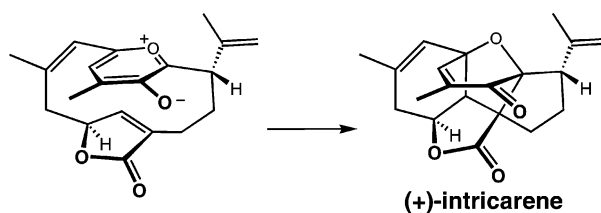# JOC*Article*

Theoretical Studies on Synthetic and Biosynthetic Oxidopyrylium−Alkene Cycloadditions: Pericyclic Pathways to Intricarene

Selina C. Wang and Dean J. Tantillo*

Department of Chemistry, University of California, Davis, One Shields Avenue, Davis, California 95616

tantillo@chem.ucdavis.edu

(+)-intricarene

Herein we describe quantum chemical calculations (B3LYP) on the intramolecular oxidopyrylium−alkene cycloadditions used in two recently reported total syntheses of (+)-intricarene, and possibly also occurring during its biosynthesis. Using theory, we address (1) the necessity of enzyme intervention if this reaction occurs in Nature and (2) the effects of substituents attached to the oxidopyrylium and alkene groups on the activation barriers for cycloaddition.

Introduction

(+)-Intricarene (**1**, Scheme 1), a recently isolated diterpenoid,[1,2] has attracted attention from experimentalists due to its unique, complex structure and potential biological activity.[3,4] In 2006, Pattenden and co-workers[3] and Trauner and co-workers[4] each reported efficient and elegant total syntheses of (+)-intricarene. The key (and final) step in both of these synthetic routes was the intramolecular oxidopyrylium−alkene cycloaddition of **2** (Scheme 1; generated from an oxidation product (**3**) of another natural product, (−)-bipinnatin J[2c,d]). Both research groups suggested that such a cycloaddition may also occur in the biosynthesis of (+)-intricarene, and the Trauner group emphasized that enzymatic intervention may be necessary to promote the formation of the oxidopyrylium zwitterion.

This unusual proposal of a biosynthetic oxidopyrylium−alkene cycloaddition,[5] coupled with the many reported applications of oxidopyrylium−alkene cycloadditions to natural prod-

ucts total synthesis[6,7] and our general interest in biosynthetic pathways to terpenoids and other polycyclic natural products,[8] prompted us to examine this transformation in detail. Using quantum chemical calculations,[9] we attempt to address these questions: (1) What is the activation barrier for the cycloaddition shown in Scheme 1; is the barrier small enough for the reaction to occur without enzymatic intervention? (2) How do the geometric constraints of the polycyclic ring system in **2**, the substituents attached to the oxidopyrylium and alkene groups, the solvent, and the temperature each contribute to the magnitude of this barrier?

Methods

GAUSSIAN03 was employed for all calculations.[10] All geometries were optimized at the B3LYP/6-31G(d) level of theory,[9,11] and some

(1) Marrero, J.; Rodríguez, A. D.; Barnes, C. L. *Org. Lett.* **2005**, *7*, 1877−1880.

(2) Related natural products: (a) Marrero, J.; Rodríguez, A. D.; Baran, P.; Raptis, R. G.; Sánchez, J. A.; Ortega-Barria, E.; Capson, T. L. *Org. Lett.* **2004**, *6*, 1661−1664. (b) Rodríguez, A. D.; Shi, Y.-P. *J. Org. Chem.* **2000**, *65*, 5839−5842. (c) Rodríguez, A. D.; Shi, J.-G.; Huang, S. D. *J. Org. Chem.* **1998**, *63*, 4425−4432. (d) Williams, D.; Andersen, R. J.; Van Duyne, G. D.; Clardy, J. *J. Org. Chem.* **1987**, *52*, 332−335.

(3) Tang, B.; Bray, C. D.; Pattenden, G. *Tetrahedron Lett.* **2006**, *47*, 6401−6404.

(4) Roethle, P.; Hernandez, P. T.; Trauner, D. *Org. Lett.* **2006**, *8*, 5901−5904.

(5) An oxidopyrylium−alkene cycloaddition has also been suggested as part of a possible biosynthetic route to the polygalolides; see: Nakamura, S.; Sugano, Y.; Kikuchi, F.; Hashimoto, S. *Angew. Chem., Int. Ed.* **2006**, *45*, 6532−6535.

(6) Seminal reports: (a) Hendrickson, J. B.; Farina, J. S. *J. Org. Chem.* **1980**, *45*, 3359−3361. (b) Hendrickson, J. B.; Farina, J. S. *J. Org. Chem.* **1980**, *45*, 3361−3363. (c) Sammes, P. G.; Street, L. J. *J. Chem. Soc., Chem. Commun.* **1982**, 1056−1057. (d) Sammes, P. G.; Street, L. J. *J. Chem. Soc., Perkin Trans. 1* **1983**, 1261−1265. (e) Sammes, P. G.; Street, L. J. *J. Chem. Res. (S)* **1984**, 196−197.

SCHEME 1

(+)-intricarene, 1
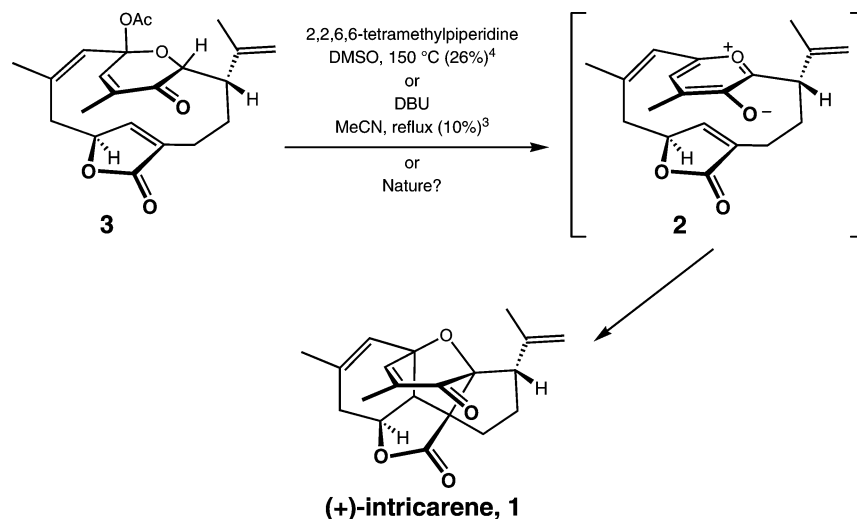
were also optimized at the B3LYP/6-31+G(d,p) and MP2/6-31G-(d)[12] levels of theory to assess whether the energy barriers vary significantly when using different methods. In addition, single-point calculations using mPW1PW91 were performed on some optimized

B3LYP/6-31G(d) and B3LYP/6-31+G(d,p) geometries.[13a] All stationary points were characterized as minima or transition structures by analyzing their vibrational frequencies (minima had only real frequencies and transition-state structures had one imaginary frequency). Intrinsic reaction coordinate (IRC) calculations were used to further characterize the identity of transition structures.[14] All reported energies (ΔE) from B3LYP/6-31G(d) calculations include zero-point energy corrections from frequency calculations, scaled by 0.9806.[15] All reported energies from B3LYP/6-31+G(d,p) calculations (ΔE) include zero-point energy corrections from frequency calculations, unscaled. "Activation barriers" ($\Delta E^{\ddagger}$) discussed in the text correspond to barriers computed based on zero-point energy corrected absolute energies. Free energy barriers ($\Delta G^{\ddagger}$, at both 25 and 150 °C) were also computed and are tabulated in the Supporting Information. In some cases, the effects of solvent (H$_2$O [ϵ = 78.39], DMSO [ϵ = 46.7], and CH$_3$CN [ϵ = 36.64]) were modeled using CPCM calculations (with UAKS radii), a self-consistent reaction field (SCRF) method.[16] Structural drawings were produced using *Ball & Stick*.[17]

As a check on the performance of B3LYP for modeling oxidopyrylium–alkene cycloadditions, we examined several simple systems described in the seminal report of Hendrickson and Farina.[6a] Shown in Table 1 are alkenes (and one alkyne) employed by these researchers in cycloaddition reactions using the parent unsubstituted oxidopyrylium. Alkenes on the left reacted to produce cycloadducts at ∼135 °C, while those on the right were described as unreactive.

(7) Selected examples of oxidopyrylium–alkene cycloadditions in natural products synthesis: (a) Sammes, P. G.; Street, L. J. *J. Chem. Soc., Chem. Commun.* **1983**, 666–668. (b) Bromidge, S. M.; Sammes, P. G.; Street, L. J. *J. Chem. Soc., Perkin Trans. 1* **1985**, 1725–1730. (c) Wender, P. A.; Lee, H. Y.; Wilhelm, R. S.; Williams, P. D. *J. Am. Chem. Soc.* **1989**, *111*, 8954–8957. (d) Bauta, W.; Booth, J.; Bos, M. E.; DeLuca, M.; Dioazio, L.; Donohoe, T.; Magnus, N.; Magnus, P.; Mendoza, J.; Pye, P.; Tarrant, J.; Thom, S.; Ujjainwalla, F. *Tetrahedron Lett.* **1995**, *36*, 5327–5330. (e) Marshall, K. A.; Mapp, A. K.; Heathcock, C. H. *J. Org. Chem.* **1996**, *61*, 9135–9145. (f) Magnus, P.; Diorazio, L.; Donohoe, T. J.; Giles, M.; Pye, P.; Tarrant, J.; Thom, S. *Tetrahedron* **1996**, *52*, 14147–14176. (g) Wender, P. A.; Rice, K. D.; Schnute, M. E. *J. Am. Chem. Soc.* **1997**, *119*, 7897–7898. (h) Baldwin, J. E.; Mayweg, A. v. W.; Pritchard, G. J.; Adlington, R. M. *Tetrahedron Lett.* **2003**, *44*, 4543–4545. (i) Krishna, U. M.; Srikanth, G. S. C.; Trivedi, G. K.; Kodand, D. D. *Synlett* **2003**, *15*, 2383–2385. (j) Snider, B. B.; Grabowski, J. F. *Tetrahedron Lett.* **2005**, *46*, 823–825. (k) Snider, B. B.; Wu, X.; Nakamura, S.; Hashimoto, S. *Org. Lett.* **2007**, *9*, 873–874.

(8) (a) Gutta, P.; Tantillo, D. J. *J. Am. Chem. Soc.* **2006**, *128*, 6172–6179. (b) Hong, Y. J.; Tantillo, D. J. *Org. Lett.* **2006**, *8*, 4601–4604. (c) Gutta, P.; Tantillo, D. J. *Org. Lett.* **2007**, *9*, 1069–1071.

(9) Previous computational papers on oxidopyrylium–alkene cycloadditions (all make use of B3LYP calculations): (a) López, F.; Castedo, L.; Mascareñas, J. L. *J. Org. Chem.* **2003**, *68*, 9780–9786 (this paper examines intramolecular oxidopyrylium–alkene cycloadditions). (b) Zaragozá, R. J.; Aurell, M. J.; Domingo, L. R. *J. Phys. Org. Chem.* **2005**, *18*, 610–615 (this paper includes calculations on intramolecular cycloadditions with both oxidopyrylium zwitterions and γ-pyrones) and references therein. (c) Krishnan, K. S.; Sajisha, V. S.; Ana, S.; Suresh, C. H.; Bhadbhade, M. M.; Bhosekar, G. V.; Radakrishnan, K. V. *Tetrahedron* **2006**, *62*, 5952–5961 (this paper examines oxidopyrylium–fulvene cycloadditions). (d) See also ref 7g for semiempirical calculations on an intramolecular oxidopyrylium–alkene cycloaddition.

(10) Frisch, M. J.; et al. *Gaussian 03*, revision B.04; Gaussian, Inc.: Pittsburgh, PA 2004.

(11) (a) Becke, A. D. *J. Chem. Phys.* **1993**, *98*, 5648–5652. (b) Becke, A. D. *J. Chem. Phys.* **1993**, *98*, 1372–1377. (c) Lee, C.; Yang, W.; Parr, R. G. *Phys. Rev. B: Solid State* **1988**, *37*, 785–789. (d) Stephens, P. J.; Devlin, F. J.; Chabalowski, C. F.; Frisch, M. J. *J. Phys. Chem.* **1994**, *98*, 11623–11627. (e) On the basis of previous studies on cycloaddition and other pericyclic reactions (which compare the B3LYP method to other methods including multiconfigurational approaches), we expect our computed activation barriers to be reliable to within a few kcal/mol, and the *relative* energies of competing transition structures to be considerably more accurate (i.e. errors in our calculations are expected to be systematic). See, for example: Guner, V. A.; Khuong, K. S.; Houk, K. N.; Chuma, A.; Pulay, P. *J. Phys. Chem. A* **2004**, *108*, 2959–2965; Guner, V.; Khuong, K. S.; Leach, A. G.; Lee, P. S.; Bartberger, M. D.; Houk, K. N. *J. Phys. Chem. A* **2003**, *107*, 11445–11459.

(12) Møller, C.; Plesset, M. S. *Phys. Rev.* **1934**, *46*, 618–622.

(13) (a) It has been suggested that B3LYP may systematically underestimate the reaction energies for cyclization reactions, and it was therefore recommended that mPW1PW91 single-point calculations may improve the energetics for such systems (Matsuda, S. P. T.; Wilson, W. K.; Xiong, Q. *Org. Biomol. Chem.* **2006**, *4*, 530–543). (b) For comparison, the relative energies of **2**, transition-state structure **2→1**, and **1** at the mPW1PW91/6-31G(d)//B3LYP/6-31G(d) level (without zero-point energy corrections) are, respectively, [0.00], 14.8, and −23.8 kcal/mol, and at the mPW1PW91/6-31+G(d,p)//B3LYP/6-31+G(d,p) level (without zero point energy corrections) are, respectively, [0.00], 15.5, and −22.2 kcal/mol.
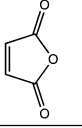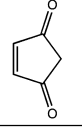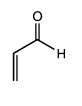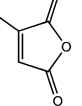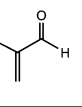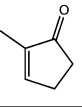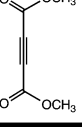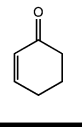
(14) (a) Gonzalez, C.; Schlegel, H. B. *J. Phys. Chem.* **1990**, *94*, 5523–5527. (b) Fukui, K. *Acc. Chem. Res.* **1981**, *14*, 363–368.

(15) Scott, A. P.; Radom, L. *J. Phys. Chem.* **1996**, *100*, 16502–16513.

(16) (a) Barone, V.; Cossi, M. J. *J. Phys. Chem. A* **1998**, *102*, 1995–2001. (b) Barone, B.; Cossi, M.; Tomasi, J. *J. Comput. Chem.* **1998**, *19*, 404–417. (c) Takano, Y.; Houk, K. N. *J. Chem. Theor. Comput.* **2005**, *1*, 70–77. (d) Aside from transition structures **2→1** and isomeric **2→1**, the geometries of all structures were optimized in the given solvent. Due to convergence problems, only single point calculations were successfully completed for the transition structures in Figure 1; consequently, barriers in solvent discussed in the text for the structures shown in Figure 1 are based only on single point energies for **1**, **2**, **2→1**, and isomeric **2→1**.

(17) Müller, N.; Falk, A. *Ball & Stick V.3.7.6*, molecular graphics application for MacOS computers; Johannes Kepler University: Linz 2000.

TABLE 1. Various Alkenes Employed by Hendrickson and Farina[6a] in Cycloaddition Reactions Using the Parent Unsubstituted Oxidopyrylium and Our Computed Activation Barriers (B3LYP/ 6-31G(d); $\Delta G^{\ddagger}$ at 135 °C)

reactive alkene/alkyne	calculated barrier $\Delta E^{\ddagger}/\Delta G^{\ddagger}$ (kcal/mol)	unreactive alkene	calculated barrier $\Delta E^{\ddagger}/\Delta G^{\ddagger}$ (kcal/mol)
	6.0/23.7		8.1/25.9
	6.7/23.9		9.3/27.6
	7.2/24.7		11.5/30.2
	7.9/25.5		12.2/30.1

Next to each structure are our computed activation barriers (B3LYP/ 6-31G(d), based on the lowest-energy transition-state structure for each system). Although some of the computed barriers are close in energy, note that all of the barriers for the unreactive alkenes are higher than those for the reactive alkenes. Moreover, the major products observed experimentally for the reactive alkenes (i.e., the result of both regiochemical and endo/exo preferences) corresponded to those resulting from the lowest-energy transition structures in our calculations (see Supporting Information for details on all transition structures). These results suggest that B3LYP is an appropriate functional for modeling oxidopyrylium–alkene cycloadditions.

Results and Discussion

Intricarene Formation. We first examined structures **2**, **1**, and the transition-state structure (**2→1**) that connects them. In Figure 1, the computed geometries of these structures are shown.[18] Our B3LYP/6-31G(d) calculations suggest that this cycloaddition has an overall exothermicity of 10.3 kcal/mol (7.7 kcal/mol in terms of free energy at 25 °C) and an activation barrier of 19.9 kcal/mol (21.7 kcal/mol in terms of free energy at 25 °C).[13,19,20] This barrier is lower (in terms of free energy[19]) than the barriers we compute for oxidopyrylium–alkene cycloadditions that were previously reported to require considerable heating (vide supra) but is higher than barriers for typical

enzyme-catalyzed reactions (~15 ± 5 kcal/mol).[21] Given the limitations of the theoretical treatment used herein,[9,13] we cannot say with certainty whether the **2→1** reaction would require enzymatic intervention in a biological setting; however, we can say that, at most, a few kcal/mol of selective stabilization for the transition structure would likely lead to a biologically useful reaction rate. In any case, it is likely that an enzyme would be required to initially generate the oxidopyrylium zwitterion and trigger the cycloaddition.

Note that the computed barriers just discussed are for the gas-phase cycloaddition (which, at best, can be considered to be a very crude model of the reaction in a nonpolar enzyme active site). Given that most biological environments are likely to be polar, we also examined the effects of a polar environment through continuum solvation calculations.[16] Only relatively small effects were observed upon inclusion of polar environments, however. For example, single-point calculations with water as solvent changed the exothermicity and barrier for the **2 → 1** reaction only slightly (to −7.0 and 21.8 kcal/mol, respectively).

We were also curious as to whether there is an endo/exo preference for this cycloaddition. The computed difference in energies (ΔE) for the **2→1** transition structure shown at the bottom left of Figure 1 and the isomeric **2→1** transition structure shown at the bottom right of Figure 1 is 4.9 kcal/mol (8.0 kcal/ mol based on single points with water), favoring the transition structure that leads to (+)-intricarene (**2→1**).[22a] Thus, there appears to be an inherent preference for the oxidopyrylium– alkene orientation that leads to the observed natural product.[22b]

Models Based on Substructures of Intricarene. In order to better understand the factors that control the barrier for the cycloaddition leading to (+)-intricarene, we looked at various combinations of oxidopyrylium zwitterions (Chart 1) and alkenes (Chart 2 and ethene) that include substituents representing various structural features present in **2**, the precursor to (+)- intricarene.

The Parent System. The simplest model system that we examined consists of unsubstituted oxidopyrylium ion **E** and ethene. This system is free of regiochemical and stereochemical complications. The calculated activation barrier for the cycloaddition of these species is 9.3 kcal/mol (21.3 kcal/mol in terms of free energy at 25 °C; the free energy barrier is of course considerably larger, primarily due to the entropy penalty associated with bringing the two reactant molecules together). The free energy barrier is comparable to that for **2**, suggesting

(18) The calculated and X-ray[1] structures of (+)-intricarene (**1**) are extremely similar (see Supporting Information for a side-by-side comparison).

(19) For comparison with systems discussed later, the free energies of activation at 150°C for the **2→1** cycloaddition, calculated at the B3LYP/ 6-31G(d) and B3LYP/6-31+G(d,p) levels, are 22.8 and 23.8 kcal/mol, respectively. At these two levels of theory, the computed overall exothermicities are 6.1 and 4.2 kcal/mol, respectively.

(20) Note that B3LYP/6-31+G(d,p) optimized structures look extremely similar to the ones shown in Figure 1 (obtained using B3LYP/6-31G(d)). The two forming C−C bonds from B3LYP/6-31+G(d,p) are 2.04 and 2.48 Å in the **2→1** transition state. The calculated B3LYP/6-31+G(d,p) barrier (20.7 kcal/mol) is slightly higher than the B3LYP/6-31G(d) barrier (19.9 kcal/mol). See Supporting Information for additional details.

(21) For leading references, see: Warshel, A.; Sharma, P. K.; Kato, M.; Xiang, Y.; Liu, H.; Olsson, M. H. M. *Chem. Rev.* **2006**, *106*, 3210−3235. Table 1 of this review lists 18 enzymatic reactions for which free energies of activation (bound reactant(s) to bound rate-determining transition-state structure) have been determined; these barriers range from 11−19 kcal/ mol. Some examples of unimolecular cases: $\Delta G^{\ddagger}$ for orotodine monophosphate decarboxylase: ~15 kcal/mol (for leading references, see: Houk, K. N.; Tantillo, D. J.; Stanton, C.; Hu, Y. *Top. Curr. Chem.* **2003**, *238*, 1−22); $\Delta G^{\ddagger}$ for chorismate mutase: 15−16 kcal/mol (Kast, P.; Asif-Ullah, M.; Hilvert, D. *Tetrahedron Lett.* **1996**, *37*, 2691−2694). See also: Garcia-Viloca, M.; Gao, J.; Karplus, M.; Truhlar, D. G. *Science*, **2004**, *303*, 186− 195; Snider, M. G.; Temple, B. S.; Wolfenden, R. *J. Phys. Org. Chem.* **2004**, *17*, 586−591; and Wolfenden, R.; Snider, M. J. *Acc. Chem. Res.* **2001**, *34*, 938−945.

(22) (a) For comparison, the difference in energy between these barriers is 6.0 kcal/mol at the B3LYP/6-31+G(d,p) level, 5.1 kcal/mol at the mPW1PW91/6-31G(d)//B3LYP/6-31G(d) level, and 5.8 kcal/mol at the mPW1PW91/6-31+G(d,p)//B3LYP/6-31+G(d,p) level. (b) Although substantial geometrical changes are required to interconvert **2** and the atropoisomer that leads to the **isomeric 2→1** transition structure (Figure 1), our preliminary calculations indicate that the transition structures along this multistep pathway are within ~5 kcal/mol of **2** (see Supporting Information for details).
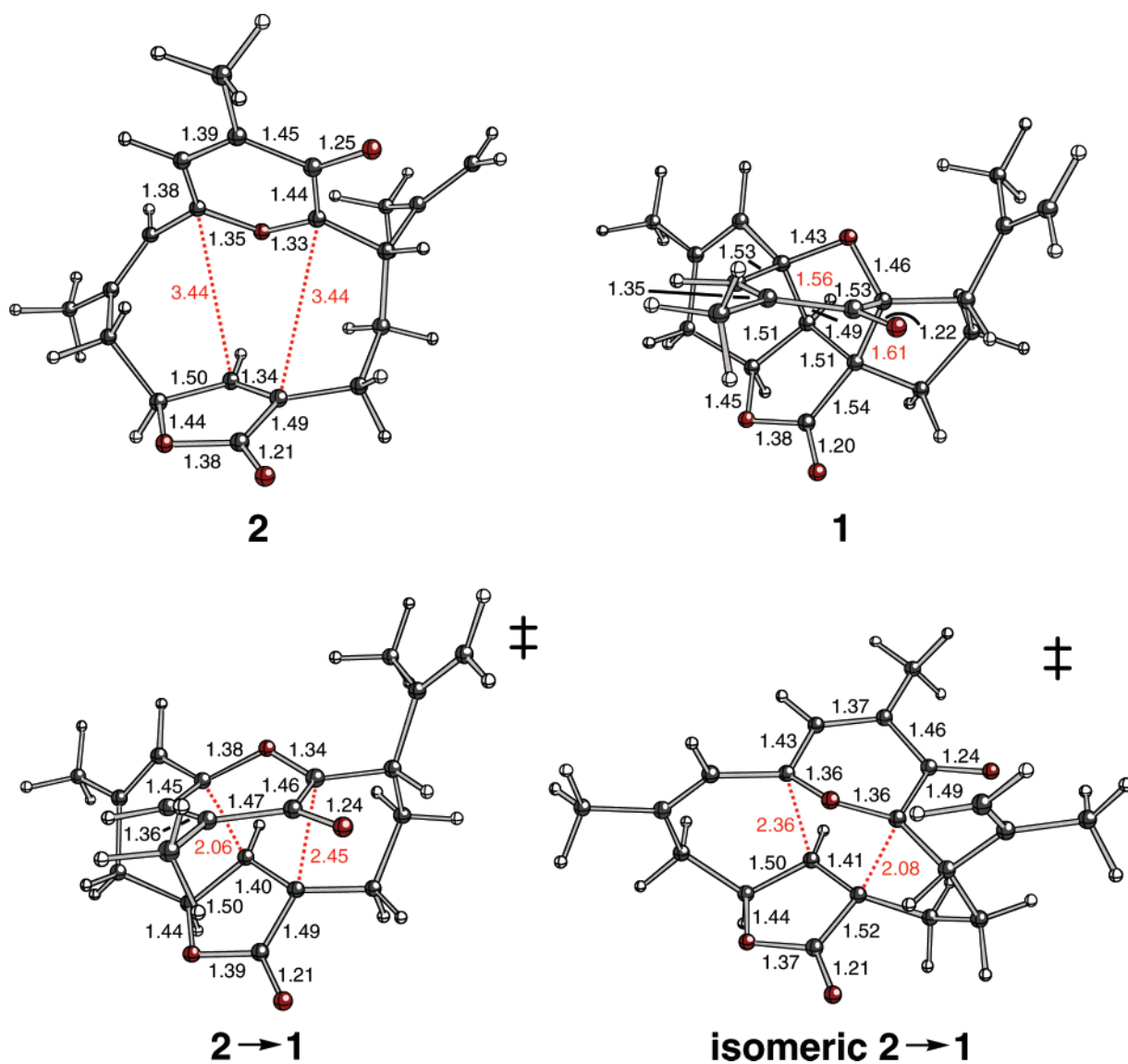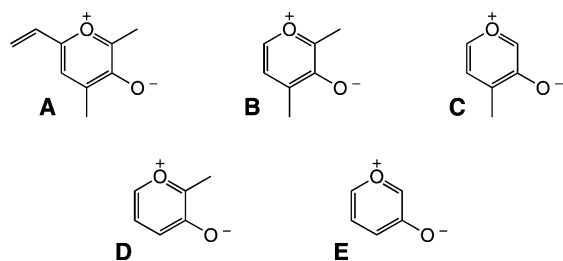
FIGURE 1. Computed geometries (B3LYP/6-31G(d), selected distances in Å) of **2**, **1**, transition-state structure **2→1,** and isomeric transition-state structure **2→1**.[18,20]

CHART 1

CHART 2

that the complexity of the intricarene precursor does not hinder this cycloaddition to any great degree. Note, however, that it does have an effect on the synchronicity of the two bond-forming events. The two C–C bonds forming in the transition structure for the **E** + ethene reaction are 2.29 and 2.42 Å long (Figure 2), while those in the **2→1** transition structure are 2.06 and 2.45 Å long (Figure 1).[20,23]

   The Simplest Cyclic Substructures. Next, consider the reaction of oxidopyrylium **E** (Chart 1) with alkene **IV** (Chart 2). The four possible transition-state structures for cycloaddition
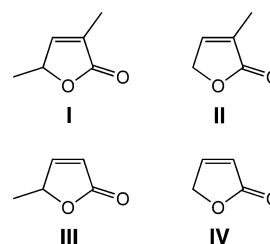
are shown in Figure 3 (transition structures in the same column lead to the same regiochemical outcome; transition structures in the same row have the same endo/exo orientation).[24] All four of the transition structures are for concerted cycloadditions, but the synchronicity of the bond-forming events for these processes varies considerably. Formation of the two new C–C σ-bonds occurs quite synchronously for **E.IV.TS2** and **E.IV.TS4**, but somewhat asynchronously for **E.IV.TS1** and **E.IV.TS3**, with **E.IV.TS3** being the least synchronous. Comparing these four transition structures to the transition-state structure for the **E** + ethene system (Figure 2), it is clear that the distances of the
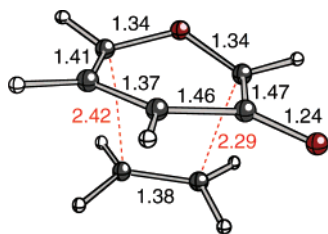
FIGURE 2. Computed geometry (B3LYP/6-31G(d), selected distances in Å) of transition-state structure for cycloaddition of **E** and ethene.

TABLE 2. Distances of Forming C−C σ-Bonds (C$_a$−C$_b$ and C$_c$−C$_d$) and Activation Barriers (Zero-Point Corrected Electronic Energies, Free Energies at 150 °C,[4] in kcal/mol and Based on Separate Reactants; B3LYP/6-31G(d)) for Transition Structures (Figure 3) for Cycloadditions of Oxidopyrylium Zwitterion E (Chart 1) and Alkene IV (Chart 2)

	C$_a$−C$_b$ (Å)	C$_c$−C$_d$ (Å)	ΔE‡ (kcal/mol)	ΔG‡ at 150 °C (kcal/mol)
E.IV.TS1	2.42	2.22	9.7	28.6
E.IV.TS2	2.33	2.31	15.3	33.5
E.IV.TS3	2.53	2.17	10.1	28.5
E.IV.TS4	2.30	2.34	12.5	30.8

forming C−C bonds in the **E** + ethene transition structure are most similar to those for **E.IV.TS1**.

Transition structures **E.IV.TS1** and **E.IV.TS3** are also lower in energy than **E.IV.TS2** and **E.IV.TS4**, and **E.IV.TS2** is the highest in energy, in terms of both enthalpy and free energy (see Table 2; for free energies, a temperature of 150 °C—that used by Trauner and co-workers[4]—was used).[25,26] This regiochemical preference (to form products with carbonyl groups far away from each other) is consistent with predictions based on the frontier molecular orbitals (FMOs) of the reactants (Figure 4)—bringing together the largest parts of the highest-energy π-type orbital of oxidopyrylium **E** (HOMO−1), and the LUMO of alkene **IV** leads to the regiochemistry corresponding to **E.IV.TS1** and **E.IV.TS3**.[27] Steric and dipole effects also contribute to the ordering of transition-state structure energies

observed. For example, **E.IV.TS2**, the highest-energy transition structure, is both sterically crowded (note the environment of the CH$_2$ group), and its two carbonyl groups are closely aligned with each other.[28] It is interesting to note that the orientation of the oxidopyrylium and alkene in this transition structure actually corresponds to the orientation leading to (+)-intricarene (compare **E.IV.TS2** and **2**→**1**).

Solvation calculations (CPCM[16]) in H$_2$O, DMSO,[4] and CH$_3$-CN[3] were also performed. While **E.IV.TS2** remains the least energetically favorable in all three solvents, the energy differences between the four transition structures decrease (down to <3 kcal/mol between the best and worse transition structures in DMSO and CH$_3$CN and down to <1 kcal/mol in water; see Supporting Information for details).[29] This is consistent with a
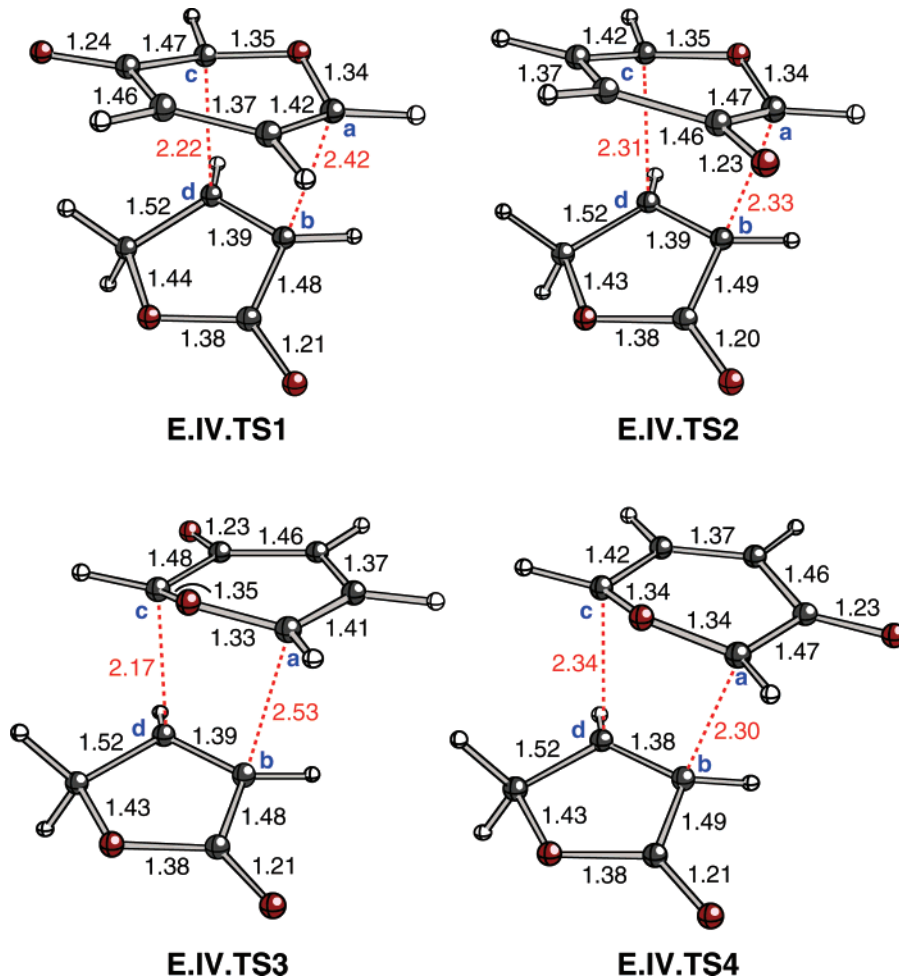

FIGURE 3. Computed geometries (B3LYP/6-31G(d), selected distances in Å) of transition-state structures for oxidopyrylium zwitterions **E** (Chart 1) and alkene **IV** (Chart 2).[24]
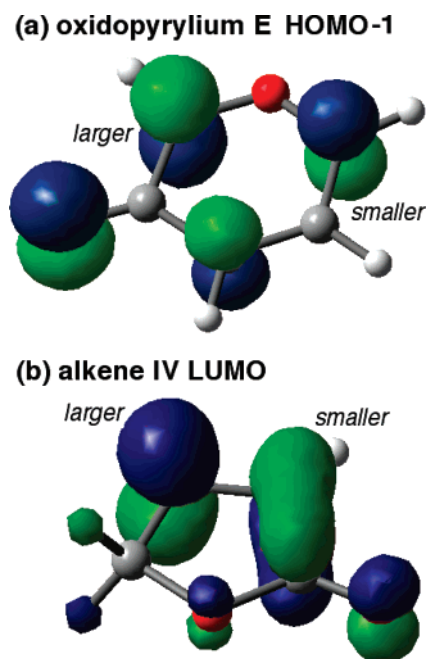
(a) oxidopyrylium E HOMO-1

larger

smaller

(b) alkene IV LUMO

larger

smaller

FIGURE 4. Frontier orbitals for **E** and **IV** (Kohn−Sham orbitals from B3LYP/6-31G(d)) in the relative orientation leading to the kinetically favored cycloaddition product. (a) HOMO−1 (the HOMO is a lone-pair type orbital) for oxidopyrylium **E**. (b) LUMO for alkene **IV**.

mitigation of the dipole effect mentioned above as the environment in which the cycloaddition occurs becomes more polar. In addition, the overall barriers for the preferred transition structures increase in more polar environments,[29] as expected for a partial "quenching" of the oxidopyrylium dipole as the cycloaddition proceeds.

Larger Substructures of Intricarene. Tables 3 and 4 list the computed barriers and distances of the forming C−C bonds in transition structures for different combinations of oxidopy-

(23) (a) We were also curious as to the role of cyclic conjugation in the oxidopyrylium zwitterions. To probe this, we looked into cycloadditions of the partially saturated **F** (a reasonable model of the 1,3-dipoles generated from the interaction of carbenes with tethered carbonyls (See, for example: Padwa, A.; Zhang, Z. J.; Zhi, L. *J. Org. Chem.* **2000**, *65*, 5223−5232 and references therein; in general, the carbene precursors to the 1,3-dipoles are generated in the presence of transition metals, and the roles of these metals in the cycloaddition are still not fully understood) and **G** with ethene. The barriers for these two cycloadditions (2.6 [14.3 kcal/mol in terms of free energy at 25 °C] and 2.8 kcal/mol [14.5 kcal/mol in terms of free energy at 25 °C], respectively) are considerably lower than those for the fully unsaturated oxidopyrylium zwitterions (9.3 kcal/mol [21.3 kcal/mol in terms of free energy at 25 °C] as described in the text). See Supporting Information for additional information on these systems (e.g., dipole moments and solvent calculations). Although these results are consistent with a loss of aromaticity for oxidopyrylium zwitterions such as **E** that is not felt by **F** or **G**, we have yet to acquire convincing computational evidence along these lines (e.g. nucleus independent chemical shifts (NICS) are not in line with this model; see Supporting Information for details).

F   **G**
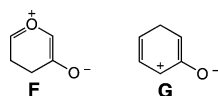
(b) One can also ask whether oxidopyrylium−alkene cycloadditions such as the **E** + ethene reaction are better described as (5 + 2) or (3 + 2) cycloadditions. Our calculations do not provide strong evidence in favor of either perspective and instead suggest that all six atoms of the oxidopyrylium group are involved in the cycloaddition. Note, for example, how the barriers change significantly when the π-system of the pyrylium ring is disrupted in either of the two manners described in ref 23a: **F** reacts as a 1,3-dipole (i.e., in a (3 + 2) cycloaddition), while **G** reacts as a 1,5-dipole (i.e., in a (5 + 2) cycloaddition).

rylium zwitterions (Chart 1) and alkenes (Chart 2). Table 3 shows the results obtained while keeping the alkene (**IV**) constant and changing the oxidopyrylium (**A**−**D**; see also Table 2 for **E**). For these systems, **TS2** (the orientations of the oxidopyrylium and alkene groups for all **X.#.TS***n* structures are analogous to those shown in Figure 1) is consistently the highest-energy transition structure. Only relatively small changes to the cycloaddition barriers are observed for oxidopyrylium zwitterions **C** and **D** compared to those for **E** (see Table 2), indicating that a single methyl substituent has only a small influence. Larger effects are observed for the more highly substituted cases **A** and **B**, however. Table 4 shows the results obtained while keeping the oxidopyrylium (**E**) constant and changing the alkene (**I**−**III**; see also Table 2 for **IV**; note that for **I** and **III**, attack from either face of the lactone can occur). Again, **TS2** is the highest-energy transition structure in most cases. However, additional steric problems occur when the methyl group on the γ-carbon of the lactone points toward the oxidopyrylium (the orientation of the corresponding alkyl group in **2**), and this effect dominates in some cases (e.g., **E.I.TS1** (Me up)).

The Advantage of Being a Macrocycle. The largest intermolecular cycloaddition that we studied involves the combination of **A** with **I** (Charts 1 and 2; Table 5). The oxidopyrylium and alkene substructures in this system bear the same sort of alkyl and alkenyl substituents present in **2**, but not tied into a ring. The transition-state structure corresponding to the orientation of the oxidopyrylium and alkene substructures for transition structure **2→1** is shown in Figure 5. It is noteworthy that the forming C−C bond distances (2.26 and 2.28 Å) in **A.I.TS2** (Me up) are quite different from the calculated bond distances in **2→1** (2.06 and 2.45 Å), which are likely a result of the geometric constraints imposed by the framework of **2**. The barrier associated with **A.I.TS2** (Me up) is approximately 30.5 kcal/mol (Δ*E*; Table 5), which is 15.2 kcal/mol higher than the barrier for **E.IV.TS2** (Table 2), primarily reflecting steric

(24) These structures and their corresponding products were also optimized with B3LYP/6-31+G(d,p) and MP2/6-31G(d), and additionally, mPW1PW91 single-point calculations were performed on the B3LYP/6-31G(d) and B3LYP/6-31+G(d,p) geometries. Qualitatively similar results were obtained at all levels, with the larger basis set and use of mPW1PW91 leading to lower overall activation barriers. For example, the activation barriers associated with **E.IV.TS1**−**TS4** at the mPW1PW91/6-31+G(d,p)//B3LYP/6-31+G(d,p) level (without zero-point energy corrections) are, respectively: 4.1, 10.4, 5.0, and 7.3 kcal/mol. See Supporting Information for energetics computed at the other levels.

(25) Energetics (Δ*E*, Δ*G* at 25°C, Δ*G* at 150°C) for all structures can be found in the Supporting Information.

(26) Counterpoise corrections for basis set superposition error (BSSE) (Simon S.; Duran M.; Dannenberg, J. J. *J. Chem. Phys.* **1996**, *105*, 11024−11031 and Boys S. F.; Bernardi, F. *Mol. Phys.* **1970**, *19*, 553−566) were calculated at the B3LYP/6-31G(d)//B3LYP/6-31G(d) and B3LYP/6-31+G-(d,p)//B3LYP/6-31G(d,p) levels. With B3LYP/6-31G(d)//B3LYP/6-31G-(d), the corrections are between 3.3−3.9 kcal/mol for transition structures **E.IV.TS1**−**TS4** and 5.6−5.9 kcal/mol for the corresponding products. With B3LYP/6-31+G(d,p)//B3LYP/6-31G+(d,p), the corrections are between 1.2−1.3 kcal/mol for transition structures **E.IV.TS1**−**TS4** and 2.6 kcal/mol for all the corresponding products. See Supporting Information for details. These results suggest that, if corrected for BSSE, the barriers discussed in the text would increase.

(27) Similar arguments based on frontier orbitals calculated using the Hückel method have been used to rationalize the regioselectivity for other oxidopyrylium−alkene cycloadditions; see ref 6e.

(28) Calculated dipole moments for **E.IV.TS1**−**TS4** are 4.3, 8.2, 1.8, and 7.7 D, respectively. Dipole moments for other structures can be found in the Supporting Information.

(29) Calculated barriers (Δ*E*‡ B3LYP/6-31G(d)) for **E.IV.TS1**−**TS4** in water: 13.6, 14.3, 13.8, 13.4 kcal/mol; in DMSO: 12.1, 14.8, 12.4, 13.6 kcal/mol; in CH₃CN: 12.1, 14.8, 12.5, 13.5 kcal/mol. See Supporting Information for geometries.

TABLE 3. Distances of Forming C−C σ-Bonds (C_a−C_b and C_c−C_d) and Activation Barriers (Zero-Point Corrected Electronic Energies, Free Energies at 150 °C,[4] in kcal/mol and Based on Separate Reactants; B3LYP/6-31G(d)) for Transition Structures for Cycloadditions of Various Combinations of Oxidopyrylium Zwitterions A−D (Chart 1) and Alkene IV (Chart 2)

|	C_a−C_b (Å)	C_c−C_d (Å)	$\Delta E^{\ddagger}$ (kcal/mol)	$\Delta G^{\ddagger}$ at 150 °C (kcal/mol)		C_a−C_b (Å)	C_c−C_d (Å)	$\Delta E^{\ddagger}$ (kcal/mol)	$\Delta G^{\ddagger}$ at 150 °C (kcal/mol)
A.IV.TS1	2.41	2.10	13.9	34.5	**C.IV.TS1**	2.44	2.20	10.3	29.4
A.IV.TS2	2.19	2.38	19.2	39.4	**C.IV.TS2**	2.28	2.35	17.0	35.4
A.IV.TS3	2.57	2.07	15.3	35.1	**C.IV.TS3**	2.52	2.15	10.8	29.1
A.IV.TS4	2.23	2.27	16.7	37.1	**C.IV.TS4**	2.32	2.31	13.3	31.6
B.IV.TS1	2.36	2.21	12.1	32.5	**D.IV.TS1**	2.33	2.24	11.8	31.5
B.IV.TS2	2.31	2.28	17.5	37.3	**D.IV.TS2**	2.36	2.25	16.1	35.0
B.IV.TS3	2.37	2.22	13.5	33.0	**D.IV.TS3**	2.37	2.23	13.0	32.2
B.IV.TS4	2.50	2.16	13.1	32.7	**D.IV.TS4**	2.49	2.18	12.5	31.5

TABLE 4. Distances of Forming C−C σ-bonds (C_a−C_b and C_c−C_d) and Activation Barriers (Zero-Point Corrected Electronic Energies, Free Energies at 150 °C,[4] in kcal/mol and Based on Separate Reactants; B3LYP/6-31G(d)) for Transition Structures for Cycloadditions of Various Combinations of Oxidopyrylium Zwitterion E (Chart 1) and Alkenes I−III (Chart 2); "Me up" Refers to Structures Where the γ-Methyl Group Is on the Face of the Alkene That Becomes Attached to the Oxidopyrylium

	C_a−C_b (Å)	C_c−C_d (Å)	$\Delta E^{\ddagger}$ (kcal/mol)	$\Delta G^{\ddagger}$ at 150 °C (kcal/mol)
E.II.TS1	2.49	2.17	12.7	32.4
E.II.TS2	2.34	2.30	19.0	38.3
E.II.TS3	2.48	2.19	15.5	34.6
E.II.TS4	2.90	2.04	11.8	30.8
E.I.TS1 (Me down)	2.47	2.18	12.9	32.6
E.I.TS2 (Me down)	2.32	2.34	23.7	43.1
E.I.TS3 (Me down)	2.93	2.05	14.0	33.4
E.I.TS4 (Me down)	2.47	2.20	15.5	35.0
E.I.TS1 (Me up)	2.39	2.25	19.1	38.7
E.I.TS2 (Me up)	2.33	2.31	19.0	38.4
E.I.TS3 (Me up)	2.90	2.04	11.7	30.6
E.I.TS4 (Me up)	2.47	2.22	17.7	37.5
E.III.TS1 (Me down)	2.42	2.22	9.8	28.9
E.III.TS2 (Me down)	2.31	2.35	18.7	37.2
E.III.TS3 (Me down)	2.53	2.18	11.8	30.8
E.III.TS4 (Me down)	2.30	2.35	12.3	30.8
E.III.TS1 (Me up)	2.34	3.04	15.3	34.0
E.III.TS2 (Me up)	2.32	2.32	15.3	33.8
E.III.TS3 (Me up)	2.53	2.17	10.0	28.5
E.III.TS4 (Me up)	2.27	2.39	13.9	32.5

TABLE 5. Distances of Forming C−C σ-Bonds (C_a−C_b and C_c−C_d) and Activation Barriers (Zero-Point Corrected Electronic Energies, Free Energies at 150 °C,[4] in kcal/mol and Based on Separate Reactants; B3LYP/6-31G(d)) for Transition Structures for Cycloadditions of Oxidopyrylium Zwitterion A (Chart 1) and Alkene I (Chart 2); "Me up" Refers to Structures Where the γ-Methyl Group Is on the Face of the Alkene That Becomes Attached to the Oxidopyrylium

|	C_a−C_b (Å)	C_c−C_d (Å)	$\Delta E^{\ddagger}$ (kcal/mol)	$\Delta G^{\ddagger}$ at 150 °C (kcal/mol)
A.I.TS1 (Me down)	2.57	2.05	17.8	39.4
A.I.TS2 (Me down)	2.28	2.22	25.1	47.0
A.I.TS3 (Me down)	2.88	2.01	17.7	38.9
A.I.TS4 (Me down)	2.43	2.10	21.1	42.5
A.I.TS1 (Me up)	2.52	2.11	25.3	46.1
A.I.TS2 (Me up)	2.28	2.26	30.5	53.4
A.I.TS3 (Me up)	2.89	2.00	23.7	45.8
A.I.TS4 (Me up)	2.46	2.10	26.8	49.0

problems in the substituted system that are accentuated in the transition structure. The barrier for **A.I.TS2** (Me up) is also 10.6 kcal/mol higher than the barrier for **2→1**, suggesting that the bulk of these steric problems are alleviated by linking the offending groups together. In terms of free energies (at 150 °C), the barrier for **A.I.TS2** (Me up) is 53.4 kcal/mol while it is
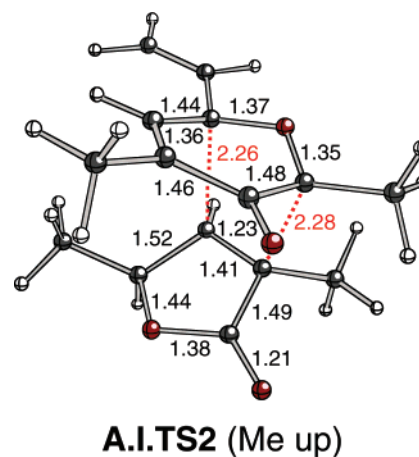
FIGURE 5. Computed geometry (B3LYP/6-31G(d), selected distances in Å) of **A.I.TS2** (Me up).

CHART 3

α–pyrone

γ–pyrone
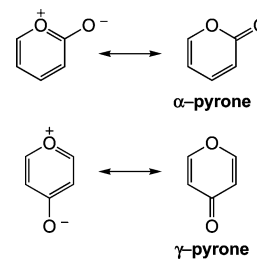
only 22.8 kcal/mol for **2→1**,[19] reflecting the additional entropy penalty for **A.I.TS2** (Me up) associated with the bimolecular nature of the cycloaddition reaction in this case. Thus, it is clear that preorganization into a ring benefits the biological system (**2**) both in terms of enthalpy and entropy.

Comparisons with Oxidopyrylium Isomers. Two isomeric forms of oxidopyrylium zwitterions have also been used in the synthesis of complex organic molecules. These (shown in Chart 3) both have uncharged resonance forms that lead to their common names: α- and γ-pyrone. The behavior of these systems is considerably different than that of the oxidopyrylium zwitterions shown in Chart 1. The thermal cycloaddition chemistry of α-pyrones with alkenes is dominated by [4 + 2] (Diels−Alder) reactions (Scheme 2a).[30] The thermal cycloaddition chemistry of γ-pyrones with alkenes appears to be restricted to reactions of γ-pyrones bearing β-OR (R = SiX₃, Ac, H) groups.[31] These systems are believed to isomerize via intramolecular R-transfer to form oxidopyrylium zwitterions before cycloaddition, and consequently they undergo the very same sorts of cycloadditions described in detail above (Scheme

(a)

(b)
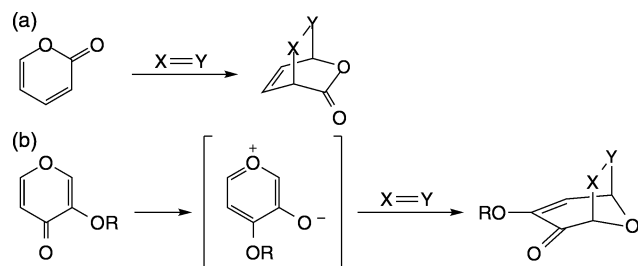
2b).[31] The need for this type of rearrangement in order to achieve efficient cycloaddition is consistent with the much higher barriers that we calculate for cycloadditions with γ-pyrones than with oxidopyrylium zwitterions. For example, the calculated barrier for the cycloaddition of unsubstituted γ-pyrone and ethene is 47.1 kcal/mol (41.9 kcal/mol in terms of free energy at 25 °C), which is much higher than that for **E** (9.3 kcal/mol [21.3 kcal/mol in terms of free energy at 25 °C]). This is likely due primarily to the separation of charge that occurs in the transition structure involving γ-pyrone. If this contention is true, then the barrier for the γ-pyrone cycloaddition should decrease in polar solvents. This barrier does indeed decrease by 5.1 kcal/mol in water (compared to the gas phase), while the barrier for the **E** + ethene cycloaddition increases by 2.3 kcal/mol.[32]

Conclusions

The two reported total syntheses of (+)-intricarene (**1**, Scheme 1) utilize an intramolecular oxidopyrylium−alkene cycloaddition of **2** as the final step.[3,4] Intrigued by the possibility that such a

cycloaddition may also occur during the biosynthesis of (+)-intricarene, we examined this transformation in detail using quantum chemical calculations. Our calculations on various combinations of model oxidopyrylium zwitterions and alkenes show that preorganization of the cycloaddition partners into a ring benefits the naturally occurring system (**2**) both in terms of enthalpy and entropy, leading to an activation barrier for the (+)-intricarene-forming cycloaddition (Scheme 1) that is calculated to be approximately 20 kcal/mol (both in terms of $\Delta E^{\ddagger}$ and $\Delta G^{\ddagger}$, and in both nonpolar and polar environments). Thus, although enzymatic intervention may be needed to generate the oxidopyrylium zwitterion, its subsequent cycloaddition would not require much, if any, additional intervention.[33]

Supporting Information Available: Additional details on calculations, including full Gaussian citation (ref 10), coordinates and energies (enthalpies and free energies at various temperatures), results of solvation calculations, computed dipole moments, and calculated NICS data on selected structures. This material is available free of charge via the Internet at http://pubs.acs.org.

JO7023762

(30) Examples of Diels−Alder reactions with α-pyrones: (a) Chen, C.-H.; Liao, C.-C. *Org. Lett.* **2000**, *2*, 2049−2052. (b) Tam, N. T.; Cho, C.-G. *Org. Lett.* **2007**, *9*, 3391−3392. (c) Shin, I.-J.; Choi, E.-S.; Cho, C.-G. *Angew. Chem., Int. Ed.* **2007**, *46*, 2303−2305. Reviews: (d) Afarinkia, K.; Vinader, V.; Nelson, T. D.; Posner, G. H. *Tetrahedron* **1992**, *48*, 9111−9171. (e) Woodard, B. T.; Posner, G. H. Recent advances in Diels-Alder cycloadditions of 2-pyrones. In *Advances in Cycloaddition*; JAI Press: Greenwich, 1999; Vol. 5, p 47.

(31) Examples of cycloadditions with γ-pyrones: (a) Volkmann, R. A.; Weeks, P. D.; Kuhla, D. E.; Whipple, E. B.; Chmurny, G. N. *J. Org. Chem.* **1977**, *42*, 3976−3978. (b) McBride, B. J.; Garst, M. E. *Tetrahedron* **1993**, *49*, 2839−2854. (c) Rumbo, A.; Castedo, L.; Mourino, A.; Mascarenãs, J. L. *J. Org. Chem.* **1993**, *58*, 5585−5586. (d) López, F.; Castedo, L.; Mascarenãs, J. L. *Org. Lett.* **2000**, *2*, 1005−1007. (e) López, F.; Castedo, L.; Mascarenãs, J. L. *Org. Lett.* **2001**, *3*, 623−625; see also refs 9a,b.

(32) (a) Calculated dipole moments for **E** and γ-pyrone are 5.1 and 3.8 D, respectively. The calculated dipole moments for their cycloaddition transition structures with ethene are 4.5 and 5.4 D, respectively. (b) Note that the wavefunction for the transition structure for the cycloaddition of γ-pyrone with **IV** is unstable (see Supporting Information), suggesting that at least some γ-pyrone cycloadditions may involve diradicals. This is not surprising in that the products of such reactions are expected to contain oxyallyl systems or cyclopropanones derived from them and cyclopropanone/oxyallyl interconversions are thought to involve diradical or diradicaloid structures in some cases; see, for example: Hess, B. A., Jr.; Eckart, U.; Fabian, J. *J. Am. Chem. Soc.* **1998**, *120*, 12310−12315.

(33) We have also computed the barriers for cycloadditions between **IV** and protonated (i.e. overall cationic) versions of **E**. Protonation on the oxygen in the ring (obviously not an inherently favorable site of protonation) lowers the cycloaddition barrier by approximately 15 kcal/mol, while protonation on the exocyclic oxygen raises the cycloaddition barrier by approximately 7 kcal/mol (in terms of free energy and for transition structures of type **TS1**). This suggests that protonation of, or hydrogen bonding to, the exocyclic oxygen in an enzyme active site (if the cycloaddition does indeed occur in an enzyme) would hinder the reaction, while protonation of, or hydrogen bonding to, the endocyclic oxygen could lead to rate acceleration. See Supporting Information for details on the computed structures.